

ORIGINAL RESEARCH

A Proteomic Atlas of Cardiac Amyloid Plaques



Taxiarchis V. Kourelis, MD,^a Surendra S. Dasari, PhD,^b Angela Dispenzieri, MD,^a Joseph J. Maleszewski, MD,^c Margaret M. Redfield, MD,^d Ahmed U. Fayyaz, MD,^d Martha Grogan, MD,^d Marina Ramirez-Alvarado, PhD,^e Omar F. Abou Ezzeddine,^d Ellen D. McPhail, MD^c

ABSTRACT

BACKGROUND In vivo mechanisms of amyloid clearance and cardiac tissue damage in cardiac amyloidosis are not well understood.

OBJECTIVES We aimed to define and quantify the amyloid plaque proteome in cardiac transthyretin amyloidosis (ATTR) and light chain amyloidosis (AL) and identify associations with patient characteristics and outcomes.

METHODS A proteomics approach was used to identify all proteins in cardiac amyloid plaques, and to compare both normal and diseased controls. All proteins identified within amyloid plaques were defined as the expanded proteome; only proteins that were enriched in comparison to normal and disease controls were defined as the amyloid-specific proteome.

RESULTS Proteomic data from 292 patients with ATTR and 139 patients with AL cardiac amyloidosis were included; 160 and 161 unique proteins were identified in the expanded proteomes, respectively. In the amyloid-specific proteomes, we identified 28 proteins in ATTR, 19 in AL amyloidosis, with 13 proteins overlapping between ATTR and AL. ATTR was characterized by a higher abundance of complement and contractile proteins and AL by a higher abundance of keratins. We found that the proteome of kappa AL had higher levels of clusterin, a protective chaperone, and lower levels of light chains than lambda despite higher levels of circulating light chains. Hierarchical clustering identified a group of patients with worse survival in ATTR, characterized by high levels of PIK3C3, a protein with a central role in autophagy.

CONCLUSIONS Cardiac AL and ATTR have both common and distinct pathogenetic mechanisms of tissue damage. Our findings suggest that autophagy represents a pathway that may be impaired in ATTR and should be further studied. (J Am Coll Cardiol CardioOnc 2020;2:632-43) © 2020 The Authors. Published by Elsevier on behalf of the American College of Cardiology Foundation. This is an open access article under the CC BY-NC-ND license (<http://creativecommons.org/licenses/by-nc-nd/4.0/>).

Transthyretin amyloidosis (ATTR) and immunoglobulin light chain amyloidosis (AL) are protein deposition diseases in which transthyretin (TTR) or clonal light chains systemically deposit as amyloid fibrils causing organ damage. Advanced cardiac involvement is the major cause of death in these patients. However, mechanisms of amyloid clearance and cardiac tissue damage in humans

From the ^aDivision of Hematology, Department of Medicine, Mayo Clinic, Rochester, Minnesota, USA; ^bDepartment of Health Sciences Research, Mayo Clinic, Rochester, Minnesota, USA; ^cDepartment of Laboratory Medicine and Pathology, Mayo Clinic, Rochester, Minnesota, USA; ^dDepartment of Cardiovascular Medicine, Mayo Clinic, Rochester, Minnesota, USA; and the ^eDepartments of Biochemistry and Molecular Biology and Immunology, Mayo Clinic, Rochester, Minnesota, USA

The authors attest they are in compliance with human studies committees and animal welfare regulations of the authors' institutions and Food and Drug Administration guidelines, including patient consent where appropriate. For more information, visit the *JACC: CardioOncology* [author instructions page](#).

Manuscript received May 25, 2020; revised manuscript received August 19, 2020, accepted August 19, 2020.

are not well understood. Amyloidogenic proteins do not exist in isolation in amyloid plaques; a large number of proteins have been identified in their “nano-environment.” Certain proteins are ubiquitous in amyloid deposits across different tissues and amyloid types and have been characterized as the “amyloid signature” proteins (1). These are serum amyloid protein, apolipoprotein E (APOE), apolipoprotein A4 (APOA4) (2), vitronectin (3), and clusterin (4). Several of these have been shown to interact with amyloid fibrils directly and modulate the extent of amyloidogenicity and/or organ toxicity (5). In addition to these well-characterized proteins, several other proteins are co-deposited in amyloid plaques and have not been adequately studied in a systematic manner. We hypothesized that the composition of the cardiac amyloid plaque proteome may provide insight into disease mechanisms in cardiac amyloidosis.

A major limitation in the accurate characterization of the amyloid proteome is that many of the non-amyloid/non-signature proteins are also abundant in the surrounding tissue. Therefore, it is difficult to accurately discern if these proteins are unique to the amyloid plaque. Studies that have evaluated amyloid proteomes have used “bulk” proteomics approaches, in which the whole tissue is analyzed, or in vitro approaches that may not reflect what is happening in vivo. The abundance of these proteins has also been largely ignored. Therefore, the exact composition and clinical significance of the amyloid plaque-specific proteome remains unknown.

In this study, using laser microdissection (LMD) of amyloid plaques followed by mass spectrometry (MS) and spectral-count-based quantification, we defined the amyloid plaque proteomes in cardiac ATTR and AL. We describe, for the first time, major patterns of protein deposition in these diseases and identify a specific proteomic signature in ATTR associated with worse clinical outcomes.

METHODS

After Mayo Clinic institutional review board approval and informed consent by patients, we identified 292 patients with cardiac ATTR and 139 patients with cardiac AL. TTR mutation status was determined by TTR gene sequencing in all except 3 cases where MS was used. Tissue samples were obtained by endomyocardial biopsy in all but 48 cases, which were obtained during autopsy. In all autopsy cases, cadavers were cooled to 4°C within 4 to 6 h from death. The median time from death to sample collection was 18 h (interquartile range: 12 to 23 h). Peptide identification was

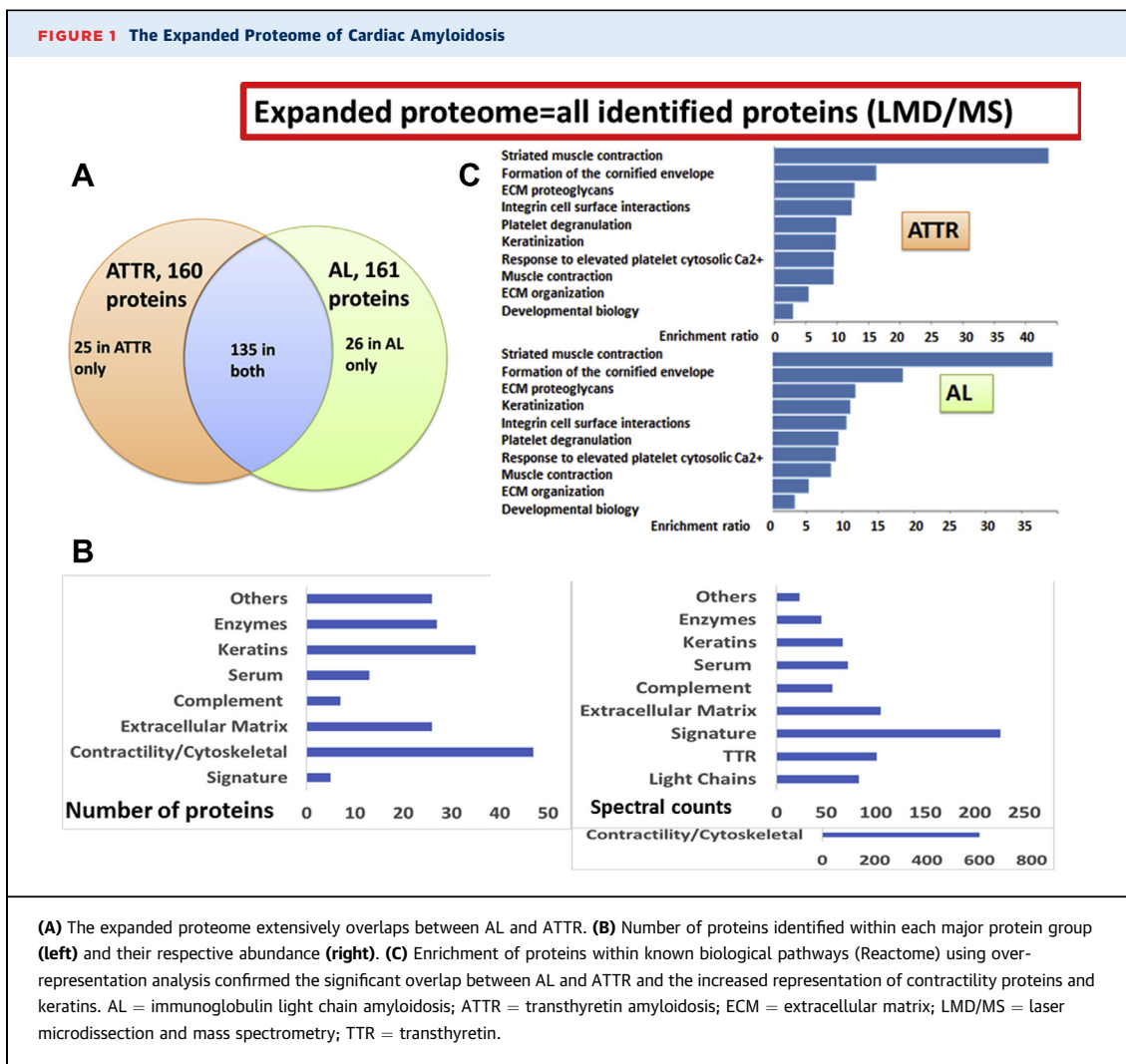
performed as previously described using LMD followed by liquid chromatography and electrospray tandem MS (LMD/MS) (6). Protein spectral counts, normalized (nSC) to the total number of spectral counts per LMD, were used as a semiquantitative measure of abundance. Controls included 6 left ventricular samples (3 from the interstitium and 3 from cardiomyocytes) obtained during autopsy from 3 patients with no known cardiac disease. In addition, we included 28 left ventricular samples (14 from the interstitium and 14 from cardiomyocytes) obtained during autopsy of 14 patients with restrictive (n = 5) or hypertensive (n = 9) cardiomyopathy. Amyloidosis was excluded in all control cases after Congo red staining. The British (7) and Mayo (8,9) cardiac staging systems were used to risk-stratify patients.

STATISTICAL ANALYSES. Statistical analyses were performed using JMP 14 (SAS Institute Inc., Cary, North Carolina). All identified proteins were considered part of the expanded amyloid proteome. Proteins were considered part of the amyloid-specific proteome if their abundance in the amyloid plaque was increased by 50% compared to normal and disease controls (cardiomyocyte and interstitium samples were pooled together) using a false detection rate (FDR) corrected $p < 0.05$.

Correlation analyses were performed using the cluster variables function of JMP. This algorithm creates groups of the most highly correlated proteins. Pearson’s R^2 was reported to assess the amount of variability explained by the covariates or cluster variabilities in a linear regression model. Hierarchical clustering was also performed in JMP using the Ward’s minimum variance method to calculate distances between clusters. Overrepresentation analyses were performed in WebGestalt (10) and using the Reactome pathway database as the functional database and an FDR-corrected $p < 0.05$ when identifying significantly overrepresented pathways. Patient overall survival (OS) was calculated from the time of diagnosis using the Kaplan-Meier method with clusters compared using the log-rank test. A Cox proportional hazards model was used to evaluate the impact of variables of interest on OS and results presented as hazard ratios with their respective 95% confidence intervals. The Fisher exact test was used to compare categorical variables and Wilcoxon rank sum (2 groups) or the Kruskal Wallis test (>2 groups) was used for continuous variables. When FDR correction was not used, a $p \leq 0.01$ was considered statistically

ABBREVIATIONS AND ACRONYMS

- AL** = light chain amyloidosis
- ATTR** = transthyretin amyloidosis
- ht** = hereditary/mutated
- LMD** = laser microdissection
- MS** = mass spectrometry
- nSC** = normalized spectral counts
- ORA** = overrepresentation analysis
- wt** = wild type



significant to account for the multiple comparisons performed.

RESULTS

The baseline characteristics of patients are shown in [Supplemental Table 1](#). The normal control patients ($n = 3$) included 2 males and 1 female age 43, 60, and 64 years, respectively. The median age for disease controls ($n = 14$) was 72 years; 12 (86%) of the controls were male to reflect the sex imbalance seen in disease samples.

THE EXPANDED PROTEOME OF AMYLOID PLAQUES IS RESTRICTED AND EXTENSIVELY OVERLAPS BETWEEN AL AND ATTR.

Excluding the amyloidogenic proteins, we identified 160 proteins in ATTR plaques and 161 in AL plaques ([Figure 1A](#), [Supplemental Table 2](#)), which we will hereafter refer to as the “expanded” amyloid proteome. Of these, 25

were unique to ATTR, and 26 were unique to AL. As a comparative metric of the expected proteomic diversity of cardiac tissue, there were several hundred distinct proteins identified in our non-amyloid control samples. We grouped proteins in the following 8 categories: amyloid signature proteins, proteins involved in muscle contraction and cytoskeletal functions, extracellular matrix and related proteins, serum complement proteins, other major serum proteins, keratins, proteins with enzymatic activity, and other proteins ([Figure 1B](#)). Keratins were not dismissed as contaminants because they were not expressed randomly across various samples, are known to be expressed in cardiac muscle, and have been shown to have protective function in some cases ([11](#)). The amyloidogenic proteins were the most abundant, followed by the amyloid signature and contractility/cytoskeletal proteins. Overall, the sum of nSC of all identified proteins in ATTR plaques was

TABLE 1 The Amyloid-Specific Proteome in Cardiac AL and ATTR

Protein	ATTR, nSC	AL, nSC	Protein	ATTR, nSC	AL, nSC
Signature Proteins			Complement Proteins		
APOA4	53 (0-292)	39 (0-352)	C3*	33 (0-166)	0 (0-57)
APOE	52 (0-263)	33 (0-283)	C9*	6 (0-58)	0 (0-119)
APCS*	62 (0-361)	18 (0-171)	CFH*	6 (0-27)	0
CLU*	29 (0-201)	16 (0-159)	CFHR1*	20 (0-89)	0 (0-20)
VTN	51 (0-333)	40 (0-431)	CFHR5*	5 (0-30)	0
Extracellular Matrix and Related Proteins			Serum Proteins		
COL1A1	15 (0-996)	14 (0-203)	APOA1*	0 (0-95)	3 (0-170)
COL1A2	11 (0-759)	11 (0-194)	APOH*	2 (0-19)	0
COL3A1*	0 (0-519)	2 (0-39)	HBG1	1 (0-53)	2 (0-13)
COL6A1*	2 (0-404)	1 (0-68)	Enzymes		
COL6A2	3 (0-339)	1 (0-50)	GPD1	0 (0-109)	0 (0-14)
CILP	0 (0-54)	0 (0-95)	PIK3C3*	0 (0-11)	3 (0-11)
DCN*	1 (0-176)	0	QSOX1*	1 (0-19)	0
FBLN1-iso-C*	18 (0-69)	0	Others		
FBLN1-iso-D*	18 (0-68)	0	AMBP*	4 (0-19)	0 (0-17)
MUC19*	0	0 (0-11)	MAGEL2*	0 (0-39)	0
PCOLCE2*	1 (0-34)	0	SERPINE2*	6 (0-67)	0 (0-16)
PRELP*	0	0 (0-34)	SHPRH*	0	0 (0-8)
PRG4*	0	0 (0-19)	SRPX*	1 (0-51)	0
TIMP3*	4 (0-22)	0 (0-60)			

Values are median (range). *Proteins differentially expressed between the 2 types (50% differential expression, FDR p value <0.05). Proteins that are part of the amyloid specific proteome [i.e., increased compared to normal and disease controls] are **bold** for ATTR, *italic* for AL, and **bold italic** overlapping proteins for both types.

AMBP = alpha-1-microglobulin/bikunin precursor; APCS = amyloid P component; APOA1 = apolipoprotein A1; APOA4 = apolipoprotein A4; APOE = apolipoprotein E; APOH = apolipoprotein H; C3, C9 = complement 3, 9; CFH = complement factor H; CFHR = complement factor H related peptide; CILP = cartilage intermediate layer protein 1; CLU = clusterin; COL = collagen; DCN = decorin; FBLN1-iso-C/D = fibulin-1 isoform C/D; GPD1 = glycerol-3-phosphate dehydrogenase 1; HBG1 = hemoglobin subunit gamma 1; MAGEL2 = MAGE family member L2; MUC19 = mucin 19; nSC = normalized spectral counts. PCOLCE2 = procollagen C-endopeptidase enhancer 2; PIK3C3 = phosphatidylinositol 3-kinase catalytic subunit type 3; PRELP = prolargin; PRG4 = proteoglycan 4; QSOX1 = quiescin sulphydryl oxidase 1; SERPINE2 = serpin family E member 2; SHPRH = NF2 histone linker PHD RING helicase; SRPX = sushi repeat containing protein X-linked; TIMP3 = metalloproteinase inhibitor 3; VTN = vitronectin.

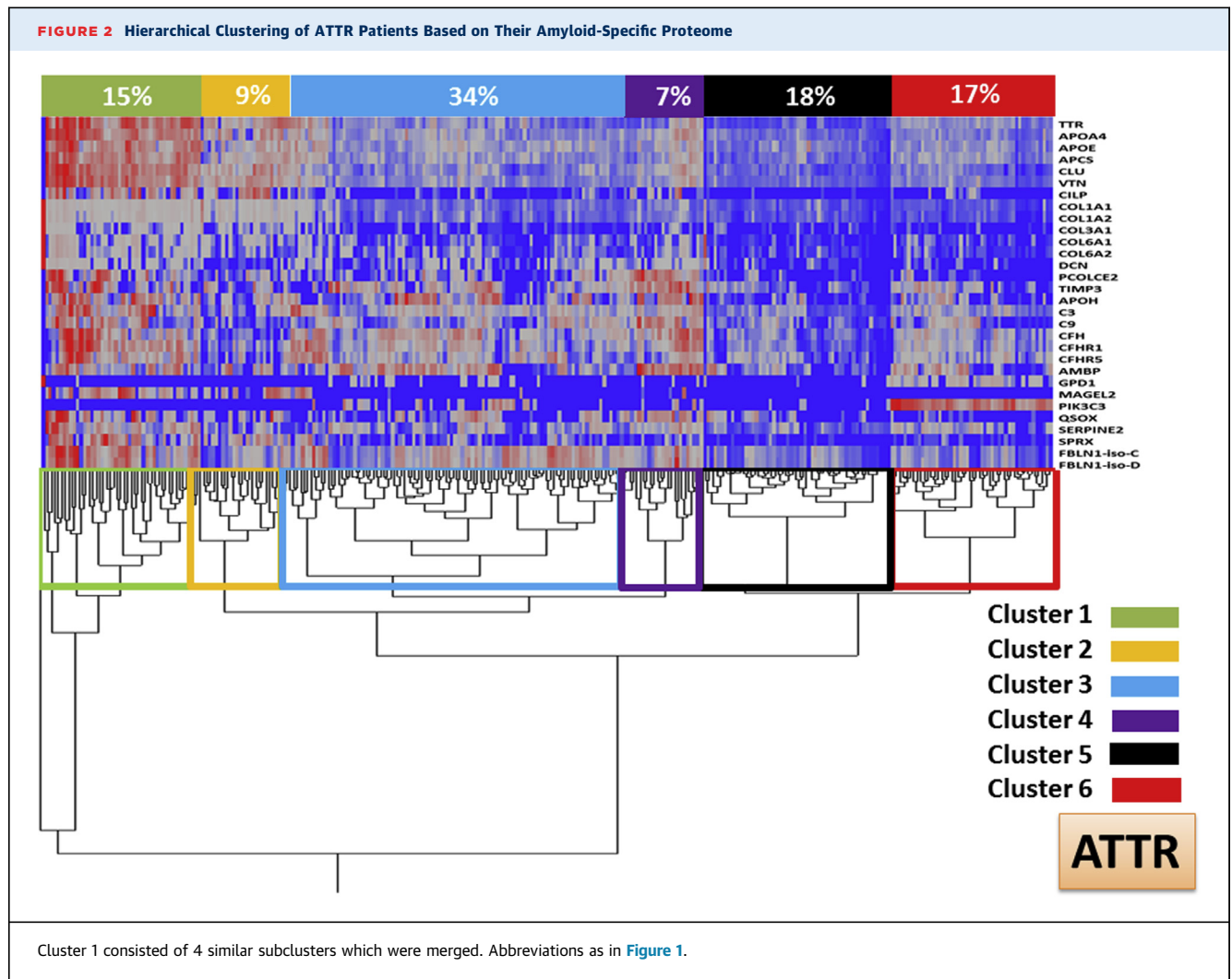
higher than that of AL (median value of 1,654 vs. 1,065; $p < 0.001$). Finally, we performed over-representation analysis (ORA) of the identified proteins in AL and ATTR to detect enrichment of proteins within known biological pathways irrespective of their abundance, confirming the overlap between the expanded proteomes of the 2 diseases (Figure 1C).

These data suggest that the amyloid plaque represents a unique proteomic “nano-environment,” with restricted proteomic diversity compared to the surrounding cardiac tissue and that ATTR amyloid plaques have a “denser” proteome than AL.

THE AMYLOID-SPECIFIC CARDIAC PROTEOME IS HIGHLY RESTRICTED. To enhance the amyloid-specific proteome identification, we considered a protein to be part of the amyloid-specific proteome only if its abundance was increased compared to both normal and disease controls. Within the expanded proteomes of ATTR and AL, several keratins were elevated in both ATTR/AL compared to diseased controls but not normal controls, and contractility/cytoskeletal proteins were elevated in both ATTR/AL compared to normal but not diseased controls

(Supplemental Tables 3 and 4); therefore, these proteins were not included. We identified 34 amyloid-specific proteins using this approach (Table 1). Specifically, 13 proteins were increased in both the ATTR and AL plaques compared to normal and diseased controls (Table 1). These include the 5 amyloid signature proteins, 4 matrix-related proteins (COL1A1, COL1A2, COL3A1, and TIMP3), 1 complement protein (CFHR1), 2 proteins involved in enzymatic processes (GPD1 and PIK3C3), and SERPINE2. Fifteen proteins were increased in the ATTR plaques only (Table 1), including 6 matrix-related proteins (COL6A1, COL6A2, CILP, DCN, FBLN1, and PCOLCE2) and 5 complement proteins (C3, C9, CFH, CFHR2, and CFHR5). In contrast, only 6 proteins were increased in AL plaques only (Table 1), including several matrix-remodeling proteins (MUC19, PRELP, and PRG4) (Supplemental Tables 3 and 4).

To investigate the possibility of sample contamination by serum, we evaluated the correlation between the concentrations of the identified serum proteins with albumin and found it to be weak (Supplemental Figure 1). The most notable difference



between AL and ATTR was that complement proteins were overrepresented in the ATTR proteome.

In aggregate, these data suggest that the 2 amyloid types may share common mechanisms of matrix remodeling (common collagen types, TIMP3, and SERPINE2) and enzymatic processes (PIK3C and GPD1) but also have several differences (complement in ATTR).

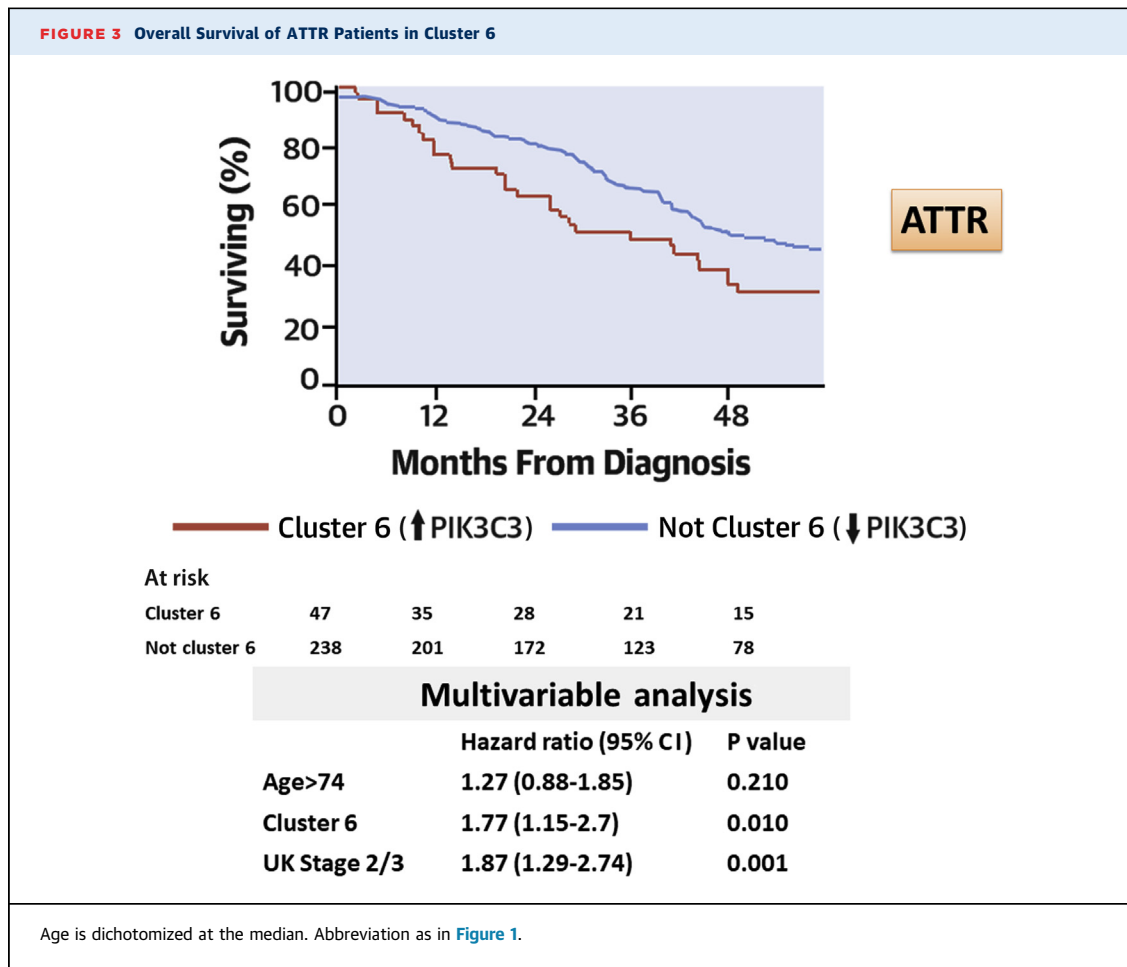
COMPLEMENT PROTEINS ARE ENRICHED IN ATTR.

We then sought to evaluate differences in amyloid-specific protein abundance according to patient clinical characteristics. For ATTR, we considered the following clinical parameters: sex, mutation status, age, and cardiac stage, and only reported differences at a $p \leq 0.01$ given the multiple comparisons performed (Supplemental Figure 2). Males had higher abundance of QSOX1 and SERPINE2 but lower APOA1 compared to females. APOH and AMBP were lower in

hereditary/mutated (ht) compared to wild type (wt) ATTR, but this was not independent of age. Elderly ATTR patients had higher levels of complement proteins and SRPX. ATTR patients with higher cardiac stage had higher levels of SERPINE2 and lower levels of the complement cascade inhibitory protein CFHR5. The same trends for CFHR5 and SERPINE2 were also noted in advanced cardiac stage patients using the Mayo staging system, but the difference did not reach our predetermined cutoff for statistical significance ($p = 0.020$ for both). No differences were noted in any of these subgroups in TTR concentrations.

THE AMYLOID-SPECIFIC PROTEOME OF AL KAPPA IS DIFFERENT FROM THAT OF AL LAMBDA.

In AL (Supplemental Figure 3), no differences in protein abundance were noted according to sex, age, or stage. SERPINE2 appeared higher in cardiac stage 3/4 patients, but this did not reach our pre-determined



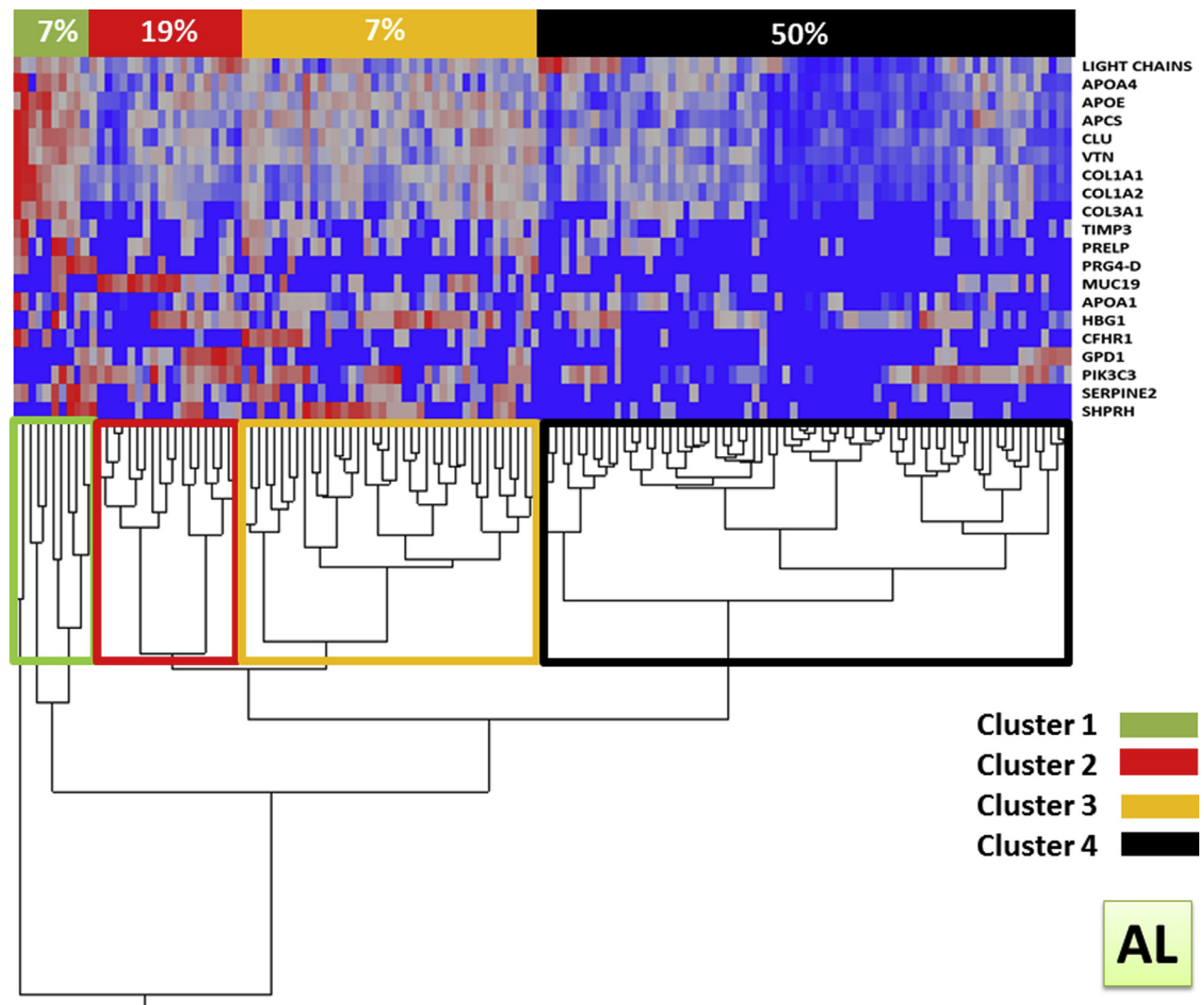
statistical significance ($p = 0.032$). When comparing kappa and lambda cases, patients with kappa AL had higher levels of clusterin (CLU), prolargin (PRELP), and SERPINE2. Kappa-restricted patients also had lower abundance of kappa light chains in their amyloid plaques compared to lambda (median nSC of 72 vs. 98; $p = 0.010$) despite having higher median difference between involved and uninvolved light chains levels in their serum (67.46 vs. 27 mg/dl; $p = 0.023$). We found no correlation between these levels and the amount of deposited light chains in AL ($R^2 = 0.008$; $p = 0.371$), which suggests that factors other than circulating light chain levels dictate their ability to seed amyloid plaques.

PROTEINS WITH SIMILAR FUNCTIONS TEND TO COEXIST IN THE AMYLOID-SPECIFIC CARDIAC PROTEOME. To identify correlations between the identified proteins, we generated a correlation matrix for the 28 ATTR amyloid-specific proteins (plus TTR) and the 19 AL amyloid-specific proteins (plus light chains) (Supplemental Figures 4 and 5) and grouped

proteins with high correlations together. Some proteins with similar functions grouped together in ATTR (e.g., signature proteins; group A, matrix proteins; group B, complement proteins; and group D). Some proteins appeared to have low correlations within their own groups, which suggest significant heterogeneity across patients. The TTR/signature protein concentration (group A) did not correlate with most collagen and matrix proteins (group B), which suggests that these are deposited in the amyloid plaque independently.

In AL (Supplemental Figure 5), correlation patterns were different. Within group A, most signature proteins correlated with collagen proteins unlike ATTR. In AL, light chains did not correlate with the remaining signature proteins. These data suggest that that light chains and signature proteins follow different deposition patterns between AL and ATTR.

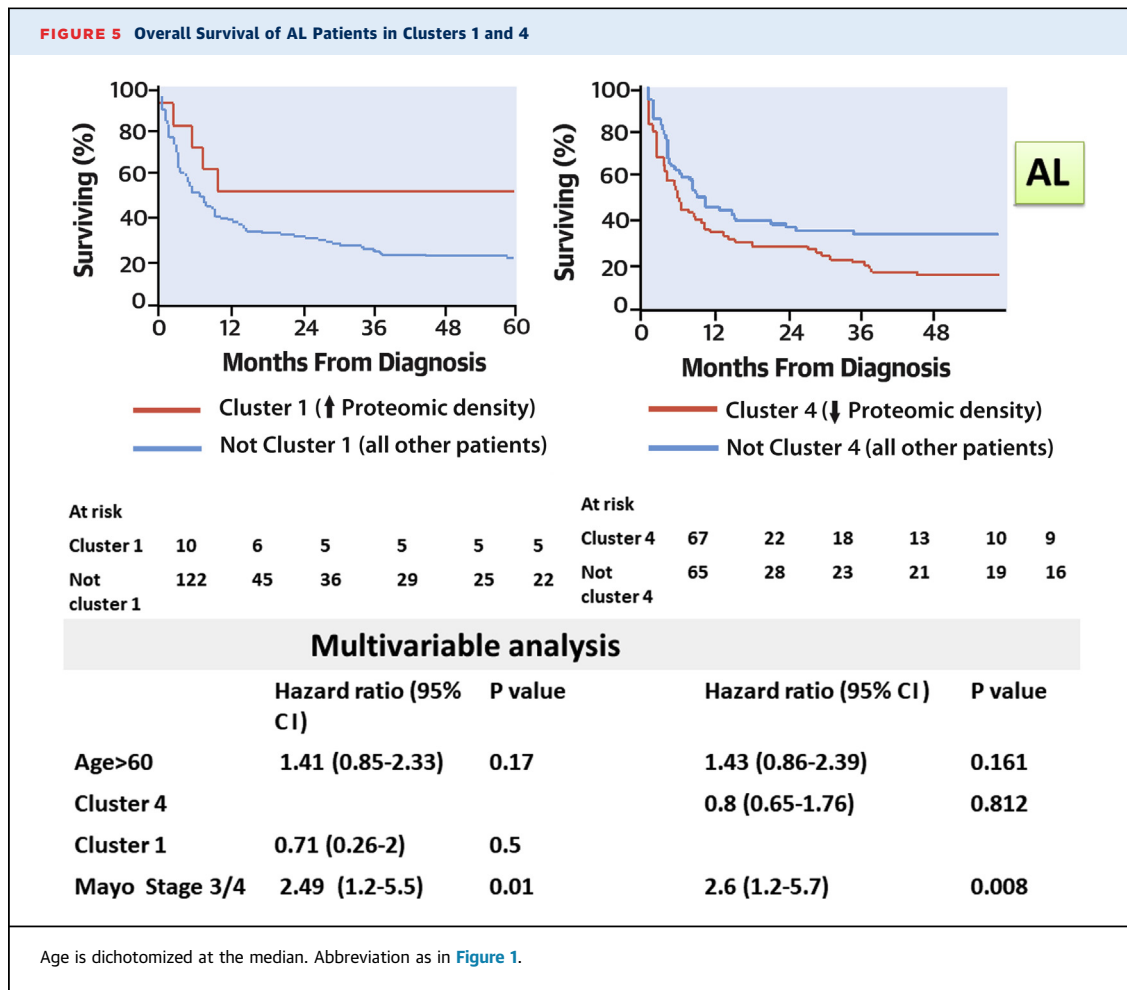
A SPECIFIC PROTEOMIC SIGNATURE IDENTIFIES PATIENTS WITH WORSE SURVIVAL IN ATTR CARDIAC AMYLOIDOSIS. Hierarchical clustering was performed

FIGURE 4 Hierarchical Clustering of AL Patients Based on Their Amyloid-Specific Proteome

Cluster 1 consisted of 3 similar subclusters which were merged.

to further clarify the patient heterogeneity identified during our correlation analyses. In ATTR, 6 distinct clusters were identified (Figure 2). Overall protein abundance was distinct across the 6 clusters and total nSC of the amyloid-specific proteome correlated with that of the expanded proteome. Most deposited proteins across these clusters followed the same overall abundance trend with some exceptions whose abundance was different than what was expected. Most complement proteins were higher in cluster 4, GPD1 and PIK3C3 were higher in cluster 6, and QSOX1 was lower in cluster 6 compared to all other clusters (Supplemental Figure 6). We then evaluated

differences in sex, mutation status, age, cardiac stage, and OS across clusters. Patients in cluster 5, the cluster with the lowest protein abundance overall, were more likely to have htATTR (36% vs. 14%; $p < 0.001$) and, as expected, be younger (median age 71 years vs. 75 years; $p < 0.001$). No difference in OS between htATTR and wtATTR was noted in this cohort. When evaluating differences in OS, patients in cluster 6 had significantly worse median OS compared to the rest of the group (36 months vs. 50 months; $p = 0.007$) (Figure 3). This effect was independent of age or cardiac stage including the Mayo cardiac staging system for ATTR.

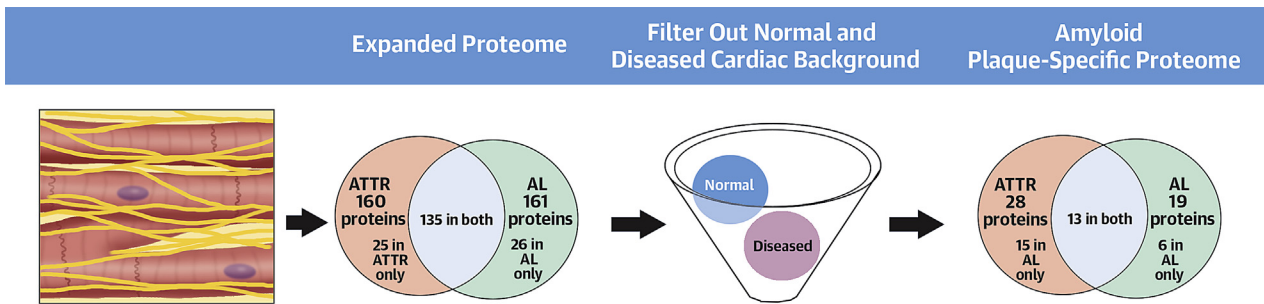


In AL, 4 distinct clusters were identified (Figure 4). Similar to ATTR, overall protein abundance was concordant between the amyloid-specific and expanded proteomes (Supplemental Figure 7A), with cluster 1 having the highest and clusters 2 and 4 the lowest protein concentrations. When considering the abundance of specific proteins within clusters, most proteins followed the overall abundance trend of amyloid-specific proteins. However, MUC19, GPD1, and PIK3C3 were the highest in cluster 2 (Supplemental Figure 7B). We then evaluated differences in sex, age, light chain restriction, cardiac stage, and OS across clusters and found no differences. Patients in clusters 4 had worse and patients in cluster 1 better median OS, respectively, compared to the rest of the group (5 months vs. 8 months, $p = 0.01$; and not reached versus 6 months, $p = 0.037$, respectively). This was independent of age but not independent of cardiac stage (Figure 5).

ORA did not show any gene pathways significantly overrepresented in the expanded proteomes of ATTR

cluster 6 compared to the rest of the cohort. However, proteins involved in keratinization, muscle contractility, and regulation of complement were underrepresented in cluster 6 (ATTR) (Supplemental Figure 8). **CONTRACTILITY AND KERATIN PROTEINS ARE INCREASED IN THE EXPANDED PROTEOMES OF ATTR AND AL, RESPECTIVELY.** Finally, we performed ORA of differentially expressed proteins from the expanded proteomes of AL and ATTR in an effort to identify potential pathogenic mechanisms that could be different between the 2 types (Supplemental Table 2). In ATTR (Supplemental Figure 9), the most overrepresented pathways included striated muscle contraction and regulation of the complement cascade. This reflects the increase of various contractility and complement proteins, respectively. In AL (Supplemental Figure 9), the most overrepresented pathways included formation of the cornified envelope (keratin proteins), apoptotic cleavage of cellular proteins (DSP, PLEC, and VIM) and E3 ubiquitin ligases (SHPRH). These data suggest

CENTRAL ILLUSTRATION Dissecting the Proteome of Cardiac Amyloid Plaques

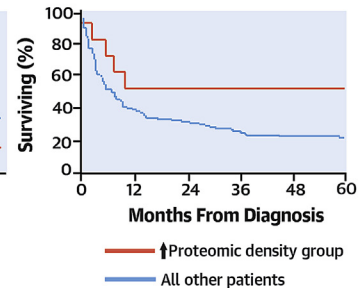
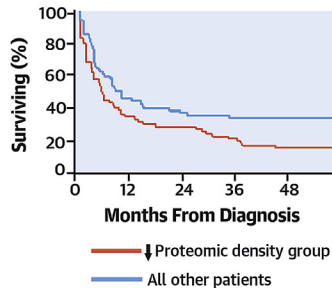
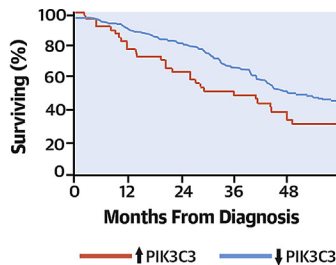


Laser microdissection/ Mass spectrometry of amyloid plaques
AL n = 153 ATTR n = 192

Correlation With Clinical Characteristics and Outcomes

- ATTR Amyloidosis**
- ↑Proteomic density compared to AL
 - ↑Complement
 - ↑Contractile proteins
 - ↑PIK3C3 → inferior survival

- AL Amyloidosis**
- ↑Keratin proteins
 - ↑Proteomic density → superior survival
 - AL kappa: ↑ protective chaperones (CLU)
 - ↓light chain seeding compared to AL lambda



Kourelis, T.V. et al. *J Am Coll Cardiol CardioOnc.* 2020;2(4):632-43.

Our findings reveal that the cardiac amyloid plaque contains a diverse spectrum of proteins and provides insights into disease pathogenesis. AL = light chain amyloidosis; ATTR = transthyretin amyloidosis; CLU = clusterin.

that muscle hypertrophy and complement activation may be dominant physiologic pathways in ATTR whereas keratin deposition may play a role in cardiac AL.

DISCUSSION

We describe, for the first time, the amyloid plaque proteome of cardiac ATTR and AL amyloidosis. We found a restricted proteomic microenvironment compared to the surrounding cardiac tissue, as well as a diverse spectrum of proteins in addition to the amyloidogenic and signature proteins. ATTR was characterized by a higher abundance of complement

and contractile proteins and AL by a higher abundance of keratin proteins, which may reflect different compensatory mechanisms between the two. We found that the proteome of kappa AL had higher levels of clusterin and lower levels of light chains despite higher circulating light chain levels. Finally, we identified a group of patients in ATTR with high levels of PIK3C3, a protein with central role in autophagy, with worse survival (Central Illustration).

The increase in contractility proteins in ATTR might reflect the increased cardiac hypertrophy noted on a gross anatomic level. These proteins were the most abundant component of the expanded proteome

in both types but were not considered part of the amyloid-specific proteome because they were increased in disease controls. Other proteins increased in ATTR included proteins involved in extracellular matrix remodeling such as DCN, FBLN1, and CILP (12-14). This might be a result of how fast cardiac tissue damage develops in AL, where these compensatory mechanisms might not have enough time to develop. The increase of QSOX1 in ATTR, an enzyme that is involved in maintaining endoplasmic reticulum homeostasis in response to misfolded proteins (15), may suggest an improved homeostatic response to misfolded TTR.

Proteins in the keratin family were present in both types but were increased in AL. Keratins were not dismissed as mere contaminants because there is evidence that they are expressed in cardiac (16) muscle and help maintain normal intercalated disk structure and mitochondrial integrity and function (11). Their absence in mouse models leads to the development of skeletal myopathies (17) and cardiomyopathy (11). In AL, their presence in amyloid plaques may reflect a more acute pattern of cardiac tissue damage, where early compensatory mechanisms are still active, and before cardiac hypertrophy and tissue remodeling mechanisms develop.

This is the first study to show increased complement deposition in ATTR plaques. Evidence of in situ (18) complement activation has been reported in heart failure in various cardiomyopathies. It is not yet understood how complement proteins impact cardiac function or associate with amyloid plaques. Our group has shown that cultured cardiomyocytes upregulate complement genes after exposure to AL fibrils (19). We also noted an increase in complement proteins with increasing age in ATTR, in agreement with what is seen with normal cardiac aging (20). Complement was not increased in the amyloid-specific proteome of AL which may be because of increased expression of complement inhibiting proteins such as CHFR1 and PRELP (21,22) or the younger age of patients.

Older ATTR patients had a distinct proteomic composition. In addition to complement proteins, levels of AMBP (23) and APOH (24), which have both been implicated in innate immunity and acute inflammation, were increased in older ATTR patients. These observations may reflect the increased generalized inflammation seen with normal aging. SRPX was also increased in elderly patients and this protein has been shown to increase amyloid deposition and toxicity in smooth muscle cells in vitro in cerebral amyloid angiopathy (25).

ATTR patients with higher cardiac stages had lower levels of CFHR5, a protein with poorly understood function with some studies reporting complement inhibition (26) and others activation (27). They also had higher levels of SERPINE2, a protein produced by fibroblasts and associated with increased cardiac fibrosis (28) and endothelial dysfunction (29). QSOX1 and SERPINE2 were both higher in ATTR male patients suggesting increased endoplasmic reticulum stress (15) and cardiac fibrosis (28), respectively.

In kappa AL patients, we noted an increase in CLU levels. CLU is an extracellular chaperone that stabilizes various misfolded proteins (30) including various types of amyloidogenic proteins (31,32). Kappa proteins are in general less thermodynamically stable than lambda proteins (33). Paradoxically, the amount of kappa light chains deposited in situ was lower, despite a higher level in the serum. So, it is possible that the increased CLU levels are associated with a higher concentration of partially folded kappa states compared to lambda. The increase of SERPINE2 and PRELP suggest that mechanisms of fibrosis (28) and cardiac remodeling (34), respectively, are different between the 2 types of AL.

We found no correlation between the total amyloid plaque protein concentration and patient survival, which suggests that amyloid tissue toxicity is not merely dictated by the amount of protein present. In fact, in AL, patients with the highest plaque protein concentration (cluster 1) fared better and those with the lowest (cluster 4) did worse. In addition, ATTR had higher overall protein abundance overall compared to AL. This suggests that proteomic abundance may serve as a surrogate of indolent disease biology.

A proteomic signature, characterized mainly by increased in PIK3C3, was associated with worse outcomes in ATTR. PIK3C3 is necessary for autophagy in the heart and other tissues (35). Light-chain-mediated dysregulation of autophagic flux in AL is critical for mediating proteotoxicity in zebrafish cardiomyocytes in vitro (36). TTR also impairs autophagy in human cell lines (37). However, this is the first study to report increase in a major autophagy marker in human hearts affected by amyloid. Autophagy has been implicated in the clearance of beta-amyloid by innate immune cells and reduction of its proteotoxicity (38,39). At the same time, autophagy induction leads to cell death which could explain the worse outcomes in this group. An intriguing finding was that in the ATTR cluster with increased PIK3C3, QSOX1, and MAGEL2 were absent and decreased, respectively. MAGEL2-null mice have been shown to have impaired autophagy (40) and this could

represent a mechanism by which autophagy fails to clear amyloid deposits in this patient group. Additionally, QSOX1 has been shown to inhibit the autophagosome-lysosome fusion in vitro (41) and might be decreased to allow the initiation of this step. The lack of a survival detriment in the high PIK3C3 cluster in AL amyloidosis could be because our study is underpowered to detect a difference. Alternatively, light chains might induce cardiac tissue damage through different pathways or inhibition of downstream autophagy signaling by proteasome inhibitors could contribute to this observation.

STUDY LIMITATIONS. Our definition of the amyloid-specific proteome was conservative. As a result, we could have excluded some proteins that were part of the amyloid-specific proteome. Despite the accuracy of LMD, the risk of sample contamination by normal tissue or nonspecific deposition of abundant proteins was still possible. In addition, we did not use the Congo red-negative tissue surrounding amyloid plaques as controls because we currently do not know the exact molecular boundary of amyloid deposition in tissues. Consequently, LMD of these areas carries the risk of including submicroscopic amyloid deposits. Another limitation is the male predominance in AL patients, which might make our results less generalizable. Furthermore, the age of the normal controls included was generally lower than that of most ATTR patients, as a result of the limited availability of normal tissues. We believe this did not affect the validity of our findings of higher complement proteins in elderly ATTR patients. Complement proteins were increased only in a specific cluster of patients and we would expect them to be uniformly increased if this was due to the inclusion of younger controls. The use of nSC as a measure of abundance has limitations as described before (42). However, this study could not have been feasible without using this relative quantification methodology because the nSC data were collected as part of clinical amyloid typing and many of the patient samples had already been returned to their referring institution. Because some cases and all controls were obtained through autopsy, some protein degradation could have occurred. However, most of these cases were processed in <24 h after death. Protein degradation is

minimal in the first 24 h for muscle and nonmuscle proteins in animals and humans, so we do not believe this influenced our results (43,44). The survival of wt versus htATTR was similar which may reflect some bias in this specific cohort. Finally, our results are in need of external validation. Given the significant heterogeneity we identified our cohort was not powered to perform internal validation of our findings.

CONCLUSIONS

Our data show that cardiac AL and ATTR have both common and distinct pathogenic mechanisms. They also suggest that autophagy represents a pathway that may be impaired and should be explored further in cardiac ATTR.

AUTHOR DISCLOSURES

This work was supported by a Mayo Clinic DLMP Research Award (008DF2019) and NIH CA186781. The authors have reported that they have no relationships relevant to the contents of this paper to disclose.

ADDRESS FOR CORRESPONDENCE: Dr. Taxiarchis V. Kourelis, Division of Hematology, Mayo Clinic, 200 First Street SW, Rochester, Minnesota 55905. E-mail: Kourelis.taxiarchis@mayo.edu. Twitter: [@taxkourelis](https://twitter.com/taxkourelis), [@adispenzieri](https://twitter.com/adispenzieri), [@marthagrogan1](https://twitter.com/marthagrogan1).

PERSPECTIVES

COMPETENCY IN MEDICAL KNOWLEDGE: The proteomic composition of amyloid plaques may have prognostic significance in patients with cardiac amyloidosis.

TRANSLATIONAL OUTLOOK: Our results serve as a framework for exploring the role of impaired autophagy in amyloid pathogenesis. Future work will focus on external validation of these results and the assessment of cardiac tissue surrounding amyloid plaques using proteomic and transcriptomic approaches. We will perform similar experiments in AL with renal involvement.

REFERENCES

- Sethi S, Theis JD, Vrana JA, et al. SH. Laser microdissection and proteomic analysis of amyloidosis, cryoglobulinemic GN, fibrillary GN, and immunotactoid glomerulopathy. *Clin J Am Soc Nephrol* 2013;8:915-21.
- Vrana JA, Theis JD, Dasari S, et al. Clinical diagnosis and typing of systemic amyloidosis in subcutaneous fat aspirates by mass spectrometry-based proteomics. *Haematologica* 2014;99:1239-47.
- Winter M, Tholey A, Kruger S, Schmidt H, Rocken C. MALDI-mass spectrometry imaging identifies vitronectin as a common constituent of amyloid deposits. *J Histochem Cytochem* 2015;63:772-9.

4. Mollee P, Boros S, Loo D, et al. Implementation and evaluation of amyloidosis subtyping by laser-capture microdissection and tandem mass spectrometry. *Clin Proteomics* 2016;13:30.
5. Wilson MR, Yerbury JJ, Poon S. Potential roles of abundant extracellular chaperones in the control of amyloid formation and toxicity. *Mol Biosyst* 2008;4:42-52.
6. Vrana JA, Gamez JD, Madden BJ, Theis JD, Bergen HR 3rd, Dogan A. Classification of amyloidosis by laser microdissection and mass spectrometry-based proteomic analysis in clinical biopsy specimens. *Blood* 2009;114:4957-9.
7. Gillmore JD, Damy T, Fontana M, et al. A new staging system for cardiac transthyretin amyloidosis. *Eur Heart J* 2018;39:2799-806.
8. Kumar S, Dispenzieri A, Lacy MQ, et al. Revised prognostic staging system for light chain amyloidosis incorporating cardiac biomarkers and serum free light chain measurements. *J Clin Oncol* 2012;30:989-95.
9. Grogan M, Scott CG, Kyle RA, et al. Natural History of wild-type transthyretin cardiac amyloidosis and risk stratification using a novel staging system. *J Am Coll Cardiol* 2016;68:1014-20.
10. Liao Y, Wang J, Jaehnig EJ, Shi Z, Zhang B. WebGestalt 2019: gene set analysis toolkit with revamped UIs and APIs. *Nucleic Acids Res* 2019;47:W199-205.
11. Papanthasiou S, Rickelt S, Soriano ME, et al. Tumor necrosis factor- α confers cardioprotection through ectopic expression of keratins K8 and K18. *Nat Med* 2015;21:1076-84.
12. Jahanyar J, Joyce DL, Southard RE, et al. Decorin-mediated transforming growth factor- β inhibition ameliorates adverse cardiac remodeling. *J Heart Lung Transplant* 2007;26:34-40.
13. Timpl R, Sasaki T, Kostka G, Chu ML. Fibulins: a versatile family of extracellular matrix proteins. *Nat Rev Mol Cell Biol* 2003;4:479-89.
14. van Nieuwenhoven FA, Munts C, Op't Veld RC, et al. Cartilage intermediate layer protein 1 (CILP1): a novel mediator of cardiac extracellular matrix remodelling. *Sci Rep* 2017;7:16042.
15. Caillard A, Sadoune M, Cescau A, et al. QSOX1, a novel actor of cardiac protection upon acute stress in mice. *J Mol Cell Cardiol* 2018;119:75-86.
16. Huitfeldt H, Brandtzaeg P. Human heart muscle contains keratin-like material in intercalated discs. *Acta Pathol Microbiol Immunol Scand A* 1984;92:481-2.
17. Stone MR, O'Neill A, Lovering RM, et al. Absence of keratin 19 in mice causes skeletal myopathy with mitochondrial and sarcolemmal reorganization. *J Cell Sci* 2007;120:3999-4008.
18. Oliveira GH, Brann CN, Becker K, et al. Dynamic expression of the membrane attack complex (MAC) of the complement system in failing human myocardium. *Am J Cardiol* 2006;97:1626-9.
19. Jordan TL, Maar K, Redhage KR, et al. Light chain amyloidosis induced inflammatory changes in cardiomyocytes and adipose-derived mesenchymal stromal cells. *Leukemia* 2020;34:1383-93.
20. Bartling B, Niemann K, Pluquet RU, Treede H, Simm A. Altered gene expression pattern indicates the differential regulation of the immune response system as an important factor in cardiac aging. *Exp Gerontol* 2019;117:13-20.
21. Happonen KE, Furst CM, Saxne T, Heinegard D, Blom AM. PRELP protein inhibits the formation of the complement membrane attack complex. *J Biol Chem* 2012;287:8092-100.
22. Birke MT, Lipo E, Adhi M, Birke K, Kumar-Singh R. AAV-mediated expression of human PRELP inhibits complement activation, choroidal neovascularization and deposition of membrane attack complex in mice. *Gene Ther* 2014;21:507-13.
23. Vyssoulis GP, Tousoulis D, Antoniadis C, Dimitrakopoulos S, Zervoudaki A, Stefanadis C. Alpha-1 microglobulin as a new inflammatory marker in newly diagnosed hypertensive patients. *Am J Hypertens* 2007;20:1016-21.
24. Matsuura E, Lopez LR, Shoenfeld Y, Ames PR. beta2-glycoprotein I and oxidative inflammation in early atherogenesis: a progression from innate to adaptive immunity? *Autoimmun Rev* 2012;12:241-9.
25. Inoue Y, Ueda M, Tasaki M, et al. Sushi repeat-containing protein 1: a novel disease-associated molecule in cerebral amyloid angiopathy. *Acta Neuropathol* 2017;134:605-17.
26. Goicoechea de Jorge E, Caesar JJ, Malik TH, et al. Dimerization of complement factor H-related proteins modulates complement activation in vivo. *Proc Natl Acad Sci U S A* 2013;110:4685-90.
27. Csincsi AI, Kopp A, Zoldi M, et al. Factor H-related protein 5 interacts with pentraxin 3 and the extracellular matrix and modulates complement activation. *J Immunol* 2015;194:4963-73.
28. Li X, Zhao D, Guo Z, et al. Overexpression of serpinE2/protease nexin-1 contribute to pathological cardiac fibrosis via increasing collagen deposition. *Sci Rep* 2016;6:37635.
29. Vidal R, Wagner JUG, Braeuning C, et al. Transcriptional heterogeneity of fibroblasts is a hallmark of the aging heart. *JCI Insight* 2019;4:e131092.
30. Poon S, Easterbrook-Smith SB, Rybchyn MS, Carver JA, Wilson MR. Clusterin is an ATP-independent chaperone with very broad substrate specificity that stabilizes stressed proteins in a folding-competent state. *Biochemistry* 2000;39:15953-60.
31. Greene MJ, Klimtchuk ES, Seldin DC, Berk JL, Connors LH. Cooperative stabilization of transthyretin by clusterin and diflunisal. *Biochemistry* 2015;54:268-78.
32. Fernandez-de-Retana S, Cano-Sarabia M, Marazuela P, et al. Characterization of ApoJ-reconstituted high-density lipoprotein (rHDL) nanodisc for the potential treatment of cerebral beta-amyloidosis. *Sci Rep* 2017;7:14637.
33. Blancas-Mejia LM, Ramirez-Alvarado M. Systemic amyloidoses. *Annu Rev Biochem* 2013;82:745-74.
34. Barallobre-Barreiro J, Didangelos A, Schoendube FA, et al. Proteomics analysis of cardiac extracellular matrix remodeling in a porcine model of ischemia/reperfusion injury. *Circulation* 2012;125:789-802.
35. Jaber N, Dou Z, Chen JS, et al. Class III PI3K Vps34 plays an essential role in autophagy and in heart and liver function. *Proc Natl Acad Sci U S A* 2012;109:2003-8.
36. Guan J, Mishra S, Qiu Y, et al. Lysosomal dysfunction and impaired autophagy underlie the pathogenesis of amyloidogenic light chain-mediated cardiotoxicity. *EMBO Mol Med* 2014;6:1493-507.
37. Teixeira CA, Almeida Mdo R, Saraiva MJ. Impairment of autophagy by TTR V30M aggregates: in vivo reversal by TUDCA and curcumin. *Clin Sci (Lond)* 2016;130:1665-75.
38. Heckmann BL, Teubner BJW, Tummers B, et al. LC3-associated endocytosis facilitates beta-amyloid clearance and mitigates neurodegeneration in murine Alzheimer's disease. *Cell* 2019;178:536-51 e514.
39. Sorrentino V, Romani M, Mouchiroud L, et al. Enhancing mitochondrial proteostasis reduces amyloid-beta proteotoxicity. *Nature* 2017;552:187-93.
40. Crutcher E, Pal R, Naini F, et al. mTOR and autophagy pathways are dysregulated in murine and human models of Schaaf-Yang syndrome. *Sci Rep* 2019;9:15935.
41. Poillet L, Pernodet N, Boyer-Guittaut M, et al. QSOX1 inhibits autophagic flux in breast cancer cells. *PLoS One* 2014;9:e86641.
42. Lundgren DH, Hwang SI, Wu L, Han DK. Role of spectral counting in quantitative proteomics. *Expert Rev Proteomics* 2010;7:39-53.
43. Choi KM, Zissler A, Kim E, et al. Postmortem proteomics to discover biomarkers for forensic PMI estimation. *Int J Legal Med* 2019;133:899-908.
44. Maleszewski J, Lu J, Fox-Talbot K, Halushka MK. Robust immunohistochemical staining of several classes of proteins in tissues subjected to autolysis. *J Histochem Cytochem* 2007;55:597-606.

KEY WORDS amyloidosis, cardiomyopathy, heart failure, proteomics

APPENDIX For supplemental tables and figures, please see the online version of this paper.